MATERIALE PLASTICE
https://revmaterialeplastice.ro
https://doi.org/10.37358/Mat.Plast.1964

Mechanics and Durability of Polyurethane Cement Composite (PUC) Material

XILONG ZHENG[1,2]*, JINSHUO YAN[3], YI WANG[3], BAITAO SUN[2], PENG LI[4]

[1] School of Civil and Architectural Engineering, Harbin University, 109 Zhongxing Road, Nangang District, Harbin, PR of China

[2] Institute of Engineering Mechanics, China Earthquake Administration, 29 Xuefu Road, Nangang District, Harbin, PR of China

[3]School of Transportation and Surveying Engineering, Shenyang Jianzhu University, 25 Hunnan Zhong Road, Hunnan District, Shenyang, PR of China

[4] Engineering Department, Shenyang Zhongyuan Traffic Investigation Design Engineering Service Co., Ltd., 888 Puhe Road, Shenbei District, Liaoning, PR of China

Abstract: *In order to investigate the mechanical properties of polyurethane cement (PUC) composite materials, axial tensile test, acid and alkali corrosion resistance test, bond test with concrete, and bond test with steel bars were conducted. The axial tensile results show that the tensile strength of PUC material is 31.11MPa, the stress-strain curve for axial tensile behavior of the material is obtained through fitting. To explore the durability of PUC materials, acid-alkali-salt corrosion resistance test is carried out, the results show that the PUC material has good resistance to acid and alkali corrosion. The failure mode of the bond test between PUC material and concrete is internal cohesion failure of concrete material, indicating good bond performance of PUC material. Axial tensile test of PUC material is carried out at different temperatures (-40℃~60℃). When subjected to temperatures between 40°C and 60°C, the strength of materials does not deteriorate. However, it is noteworthy that the material's ability to withstand tensile strain significantly increases as temperatures rise to 60°C. The bonding strength between PUC material and steel bar increases with an increase in protective layer thickness, and at a thickness of 70 mm, the maximum bond stress is achieved at 16.38 MPa. On the other hand, the strength of the bond reduces as the anchorage length increases. Smooth round bars demonstrate a significantly lower bond strength compared to deformed bars, as their maximum bond strength is at approximately 47.4% of that of the deformed bars under the same conditions.*

Keywords: *Polyurethane cement composite (PUC) material, mechanical properties, bond strength, durability, Pull-out test*

1. Introduction

Bridges are an essential part of highway transportation and play a vital role in the transportation industry. With the continuous development of the economy and the increasing traffic volume, the bridges as the lifeline of highway transportation are irreplaceable [1, 2]. As the economy grows, the vehicle load and traffic volume have significantly increased [3]. Additionally, natural factors such as acid rain, air, and temperature have led to a series of structural damages in bridges, including loading-induced cracks and concrete deterioration, resulting in a decrease in the carrying capacity of the bridges and posing a threat to their long-term operation [4, 5].

An appropriate reinforcement method for bridges with insufficient carrying capacity can extend their service life, avoiding the need for costly reconstruction [6]. The large-section method is a traditional reinforcement method with simple construction, but it has a long construction and maintenance period, a significant increase in self-weight, and a substantial impact on traffic. The use of externally bonded Fiber Reinforced Polymer (FRP) is a construction method that boasts a simple installation process and minimal impact on the pre-existing structure [7]. However, this method only offers limited structural stiffness enhancement due to the thinness of the carbon fiber cloth or sheets used, which also entails a

**email: zhengxilong88@163.com*

rather high material cost. The use of external prestressing reinforcement can significantly improve the carrying capacity and stiffness, but the construction process is complex, and the construction period is long [8-11].

Polyurethane cement composite material is an innovative type of composite material that exhibits several notable advantages [12-15]. These include high strength, exceptional toughness, and the ability to cure rapidly [17-21]. This paper presents a new method of applying PUC material to bridge reinforcement. If PUC material is used in bridge structure reinforcement, it is necessary to study its performance. Firstly, the PUC material is located in the tension area of bridge beam, and it is necessary to explore the tensile properties of the material, the bonding properties with concrete, and the bonding properties with steel bars. Secondly, the reinforced bridge is subjected to different temperatures in the service environment, so it is necessary to study the mechanical properties of PUC material at high temperatures. Finally, in order to explore the durability of PUC-reinforced beams, it is necessary to study the acid and alkali corrosion resistance of PUC material. Therefore, the tensile properties of PUC material, the bond properties with concrete, the bond properties with steel bars, the tensile properties under high temperature and the acid and alkali corrosion resistance are studied in this paper.

2. Material and methods

2.1. Material

PUC material is a type of polymer concrete material, primarily composed of black material and white material. The black material is isocyanate, while the white material is polyether polyol. The polyurethane material is formed by polymerizing the black material and white material. PUC material exhibits excellent wear resistance, strong mechanical properties, adhesion, and moldability. The raw materials for PUC material undergo a polymerization reaction when mixed according to a specific mass ratio. In the mix design, the main raw materials are polyols, isocyanates, and cement, with silicone oil acting as a catalyst, as shown in Table 1. The production process of polyurethane cement is illustrated in Figures 1 and 2.

Table 1. Composition of polyurethane cement

Polyurethane cement	Percentage（%）
Polyether polyols	24
Isocyanate	25-26
Silicone oil	0-1
Cement	50

Figure 1. Mixing process of PUC material

Figure 2. Pouring process of PUC material

2.2. Methods

2.2.1. Axial tensile test of PUC material

The axial tensile specimen was a dumbbell shaped specimen with a size of 160 mm (length) × 40 mm (width) × 10 mm (thickness), as shown in Figure 3. The tensile test was conducted by utilizing a universal testing machine that applies force at a rate of 30 N/s. Electrical resistance strain gauges and

strain acquisition boxes were employed to collect the strain of the PUC material during the tensile process, aiming to explore the strain variation of the material during the tensile process.

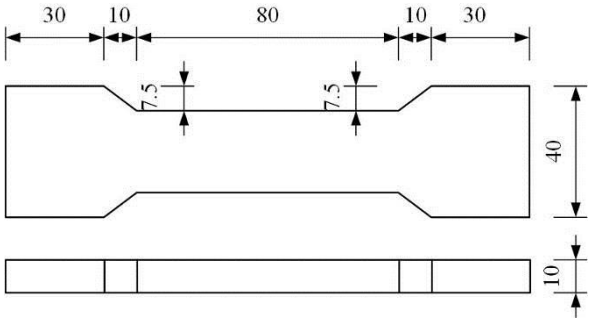

Figure 3. Dimensions of PUC material axial tensile specimen (unit: mm)

2.2.2. Direct tensile bond test between PUC and concrete

The concrete cubic specimen was cut into smaller cubic blocks with dimensions of 100 mm× 100 mm× 100 mm. A chipping hammer was used to remove the surface mortar of the concrete, exposing the sand and stone aggregates. A rectangular wooden template with dimensions of 50 mm× 50 mm was placed on top of the concrete block, aligning it with the center of the block. The bolt was placed inside the template. The process began with pouring PUC material into a template. After a period of 7 days, the wooden template was removed, as depicted in Figure 4. The concrete block of the specimen was then inserted into a specially designed fixture. The fixture rod was positioned upwards, while the specimen screw was placed downwards. To perform the tensile test, the fixture with the specimen was positioned on the tension testing machine. Throughout the tensile test, the ultimate tensile force of the test specimen was recorded and measured.

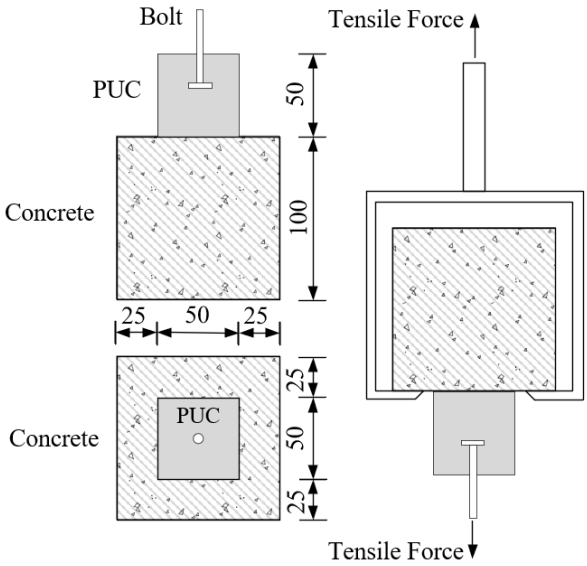

Figure 4. Direct tension bond test specimen design (unit: mm)

2.2.3. Flexural bond test between PUC and concrete

The flexural bond strength between polymer concrete and concrete was measured. Cut concrete blocks with 70mm× 70mm× 70mm were placed in a three-point steel mold. The PUC material was poured at the center of the specimen, with a height of 60 mm. The specimen's dimensions were presented in Figure 5. A universal testing machine with a distance of 160 mm between two supports was employed

to apply a three-point bending load. The loading point was positioned 80 mm away from the two supports. Before formal loading, a preloading of 50 N was applied to eliminate residual stress in the specimen.

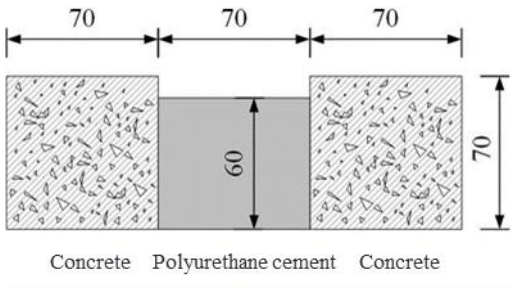

Figure 5. Size of the flexural bond test specimen (unit: mm)

2.2.4. Acid and alkali influence test

Two residual samples of PUC material from the flexural strength test were selected for acid and alkali influence testing with a length of approximately 80 mm and a width of 40 mm× 40 mm. The surface of the specimens was ground using an angle grinder to expose the content material for the determination of chemical corrosion resistance. Low and high concentration acid and alkali solutions were prepared as follows:

Hydrochloric acid (HCl) was used as the acid solution, with concentrations of 4 and 18% (vol/vol). Potassium hydroxide (KOH) was used as the alkali solution with concentrations of 30 g/L and 100 g/L.

The specimens were dried in an oven at a temperature of 100 ± 5^{o}C for two consecutive weighing, and the weight difference was not greater than 0.02 g. The tests were then conducted at room temperature. The specimens were immersed in the acid or alkali solutions contained in a beaker until a depth of 30 mm was reached. The beaker was covered with a lid, as shown in Figure 6. After 12 days of immersion, the specimens were removed and rinsed with flowing water for 5 days. They were then completely immersed in boiling water for 30 min and removed, gently wiped with a damp chamois, and dried in a drying oven at 100 ± 5^{o}C.

Figure 6. Chemical corrosion resistance determination

2.2.5. Environmental temperature impact test

To explore the effects of natural environmental temperatures on the tensile mechanical properties of the PUC material, a temperature range from -40 to 60°C was chosen for testing, to replicate the natural environmental temperature conditions. The tests were conducted at temperatures of -40, -20, 0, 20, 40, and 60°C respectively. The specimens used for the tensile test were dumbbell-shaped specimens with dimensions of 160 mm × 40 mm and a thickness of 10 mm. The narrowest width at the center of the specimen was 20 mm. The specimens used for the test are shown in Figure 7. The figure of the tensile tests at different temperatures is shown in Figure 8.

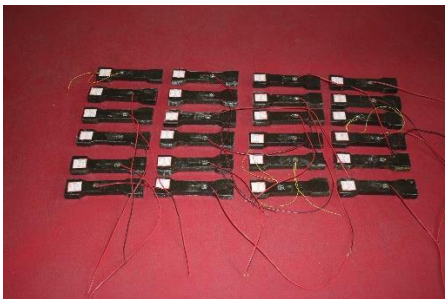

Figure 7. Dumbbell-shaped specimen

Figure 8. Tensile test at different temperatures

2.2.6. Polyurethane cement and reinforcement pull-out test

The pull-out test was performed using a wooden template. The steel bar was inserted into the rectangular wooden template, with the center of the steel bar aligned with the center of the template, and with exposed lengths of 50 mm and 300 mm on either side of the steel bar. The internal dimensions of the template were 150 mm× 150 mm× 150 mm. The PUC material was poured into the template, and after the specimen hardened, the template was removed. The specimen dimensions are shown in Figures 9 and 10.

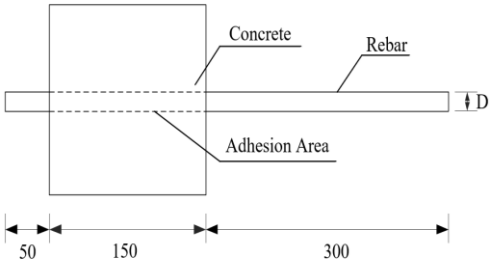

Figure 9. Detailed drawing of the specimen (unit: mm) D - steel bar diameter

Figure 10. Pouring of the specimen illustration

3. Results and discussions

3.1. Axial tensile test of PUC materials

Table 2 provides data indicating that the PUC material demonstrates an axial tensile strength of 31.11 MPa. Interestingly, despite its brittle failure mode, the material exhibits commendable ductility. The material's tensile modulus of elasticity ranges from 4300 MPa to 5600 MPa.

Table 2. Axial tensile strength of PUC material

Number	ZL01	ZL02	ZL03	ZL04	ZL05	ZL06	Average
Strength (MPa)	29.9	32.9	32.1	31.1	30.8	29.9	31.11

Based on the collected force-time and strain-time relationships during the tensile process, the stress-strain constitutive relationship curve of the axial tensile test is plotted, as well as the average stress-strain constitutive relationship curve, as shown in Figure 11 and Figure 12.

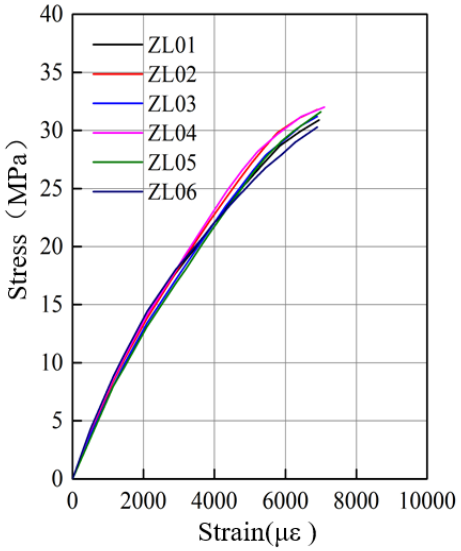

Figure 11. Axial tensile stress-strain constitutive relationship curve

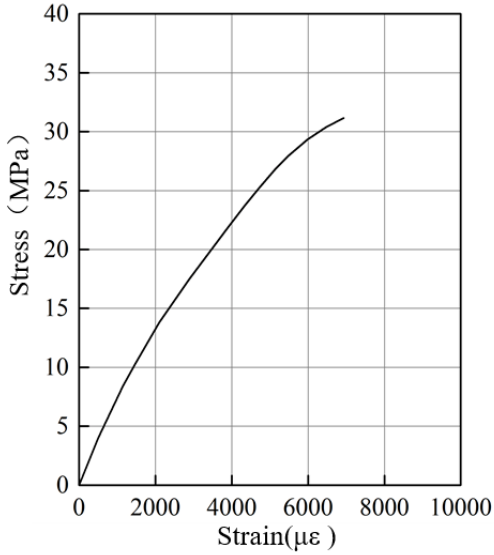

Figure 12. Axial tensile stress-strain constitutive relationship curve (Average)

The stress-strain relationship of the axial tensile specimen fits with a constitutive relationship curve, as shown in Figure 13. The constitutive curve of the PUC material is relatively smooth, and the fitting formula is as follows:

$$\sigma = 0.496 + 6977.3\varepsilon - 365682.2\varepsilon^2 \quad (1)$$

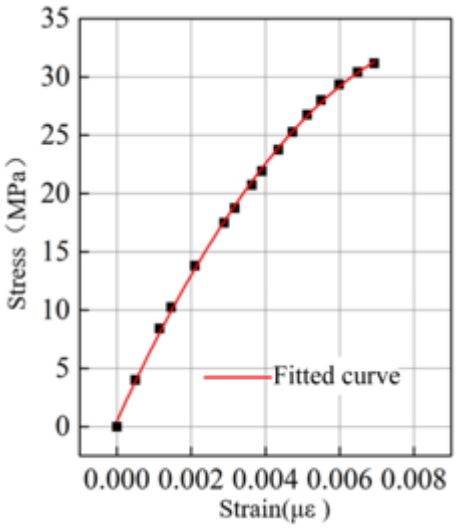

Figure 13. Fitted curve of axial tensile constitutive relationship

3.2. Direct tensile bond test results between PUC and concrete

Table 3. Bond strength of PUC material

Number	ZN01	ZN02	ZN03	Average
Strength (MPa)	3.46	3.56	3.66	3.56

Equation 2 enables the calculation of the axial bond strength between the PUC material and concrete.

$$\sigma = \frac{F}{ab} \quad (2)$$

In the equation:

F - represents the ultimate tensile force of the specimen;
a - represents the length of the contact surface between polyurethane cement and concrete;
b - represents the width of the contact surface between polyurethane cement and concrete.

The experimental results of the direct tensile bond strength between PUC material and concrete is shown in Table 3. The bond strength exceeds the cohesive force of the concrete material itself. Consequently, the failure mode observed is a cohesive failure within the concrete, with a failure stress of 3.56 MPa. Throughout the tensile process, the bond failure occurs within the concrete material itself, as depicted in Figures 14. Notably, the failure interface does not occur at the bond surface between the concrete and PUC material, indicating excellent adhesion of the PUC material.

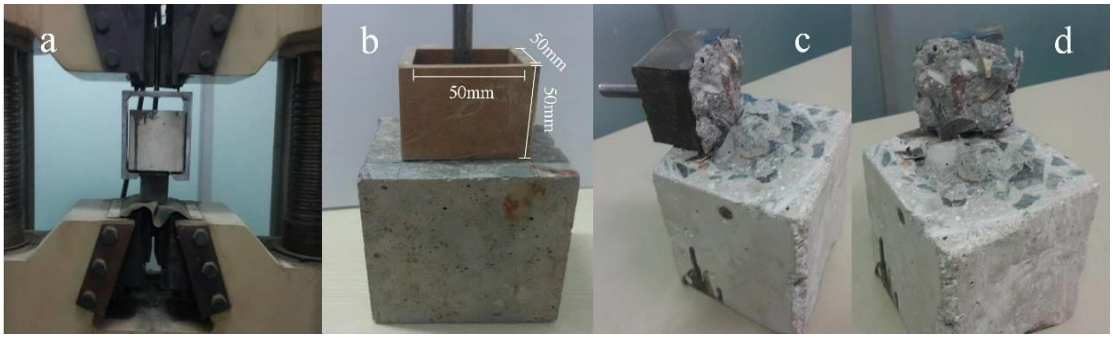

Figure 14. Direct tensile bond test (unit: mm)

3.3. Flexural bond test results between PUC and concrete

The calculation of the axial tensile bond strength between PUC material and concrete is performed using equation 3:

$$\sigma = \frac{3F(l-a)}{bh^2} \quad (3)$$

In the equation:

F - the flexural failure force of the specimen;
l - the distance between the two supports during loading;
a - the longitudinal length of the polyurethane cement in the specimen;
b - the transverse width of the polyurethane cement in the specimen;
h - the height of the polyurethane cement in the specimen.

Table 4. Bond strength of PUC material

Number	WN01	WN02	WN03	Average
Strength (MPa)	3.15	3.08	3.25	3.16

The test results of bending bond between PUC material and concrete are shown in Table 4. The bond strength between the PUC material and concrete exceeds the cohesive strength of the concrete, leading to cohesive failure within the concrete itself. The measurement of failure stress recorded a value of 3.16 MPa. Notably, the failure interface does not occur at the interface between the concrete and PUC material, indicating strong bonding characteristics of the PUC material. Flexural bond test is shown in Figure 15.

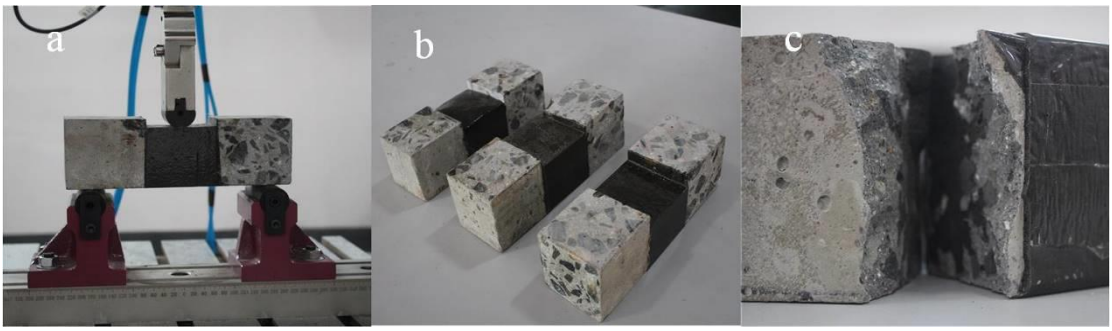

Figure 15. Flexural bond test

3.4. Acid and alkali influence test

The findings of the chemical corrosion resistance test conducted on the polyurethane cement composite material is shown in Table 5. The material is immersed in solutions containing varying concentrations of HCl and KOH. The experiment focuses on monitoring any alterations in mass. Remarkably, no visible changes are observed on the surface of the PUC material throughout the test duration. The mass loss rate in the acid solution ranges from 0.135 to 0.139 %, while in the alkali solution, the mass loss rate ranges from 0.191 to 0.307 %.

Table 5. Chemical corrosion resistance test

Number	Solution	Initial mass	Mass before testing	Mass after testing	Mass loss	Mass loss rate (%)	Corrosion resistance grade
LS	3% HCl	93.45	93.44	93.31	0.13	0.139	ULA
HS	18% HCl	81.74	81.61	81.50	0.11	0.135	UHA
LJ	30g/L KOH	94.21	94.18	94.00	0.18	0.191	ULA
HJ	100g/L KOH	75.04	74.96	74.73	0.23	0.307	UHA

3.5. Environmental temperature impact test results

The axial tensile stress-strain curves at different temperatures are shown in Figure 16. From the graph, it can be observed that, within the temperature range of -40 to 60°C, the ultimate strength of the material does not decrease. As the temperature rises, there is a mild enhancement in the ultimate tensile strain of the PUC material. This effect is particularly pronounced at 60°C, where a more noticeable increase in tensile strain is observed.

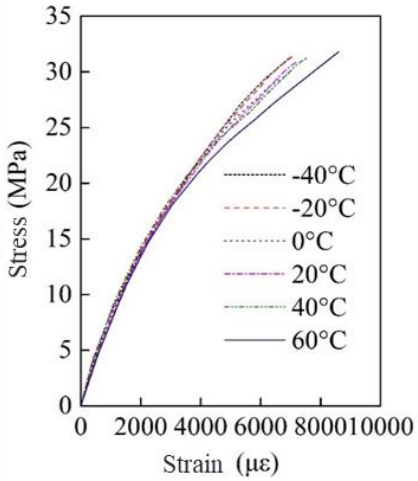

Figure 16. Axial tensile stress-strain curves at different temperatures

3.6. PUC material and steel bar pull-out test

3.6.1. Thickness of protective layer

The study involved conducting pull-out tests on threaded steel bar with a diameter of 16 mm. Three sets of pull-out specimens were used, while the protective layer thickness of the steel bar varied. The protective layer thicknesses considered were 40 mm, 50 mm, 60 mm, and 70 mm. The pull-out bond stress was calculated based on the applied pulling force to explore the effect of the protective layer thickness on the adhesive anchoring performance. The comparison of bonding stress under different protective layer thicknesses is shown in Figure 17. The average bonding stress diagram is shown in Figure 18. As the primary failure mode of the threaded steel bar is splitting, a thicker protective layer provides greater resistance against splitting. For the PUC specimens, increasing the protective layer thickness helps limit the expansion of splitting cracks or even prevent their occurrence, although this limitation has its limits. The data in the figures demonstrate that the bonding strength increases as the protective layer thickness increases. For example, when the protective layer thickness is 40mm, the stress is 10.53 MPa. This value increases to 12.36 MPa, representing a 17.38 % increase, when the protective layer thickness is 50mm. Similarly, with a protective layer thickness of 60 mm, the average bonding stress further increases to 14.00MPa, showing a 13.27% increase compared to the 50 mm thickness. Lastly, a protective layer thickness of 70 mm results in an average bonding stress of 16.38 MPa, which is a 17.00 % increase compared to the 60 mm thickness.

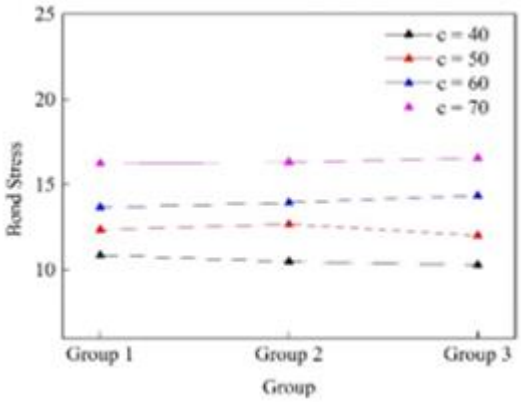

Figure 17. Comparison of bonding stress (Different thicknesses of protective layer)

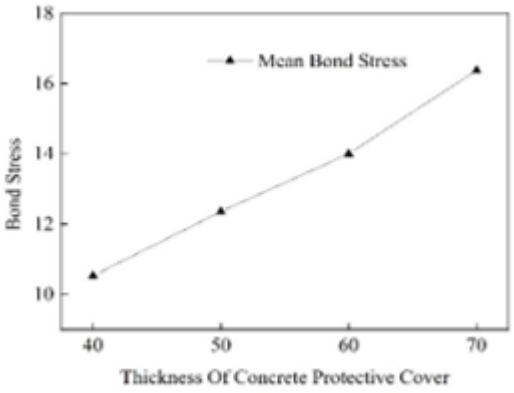

Figure 18. Average bonding stress diagram

3.6.2. Length of Reinforcement Anchorage

Comparative chart of bond stresses is shown in Figure 19, and average bond stress graph is shown in Figure 20. The pull-out tests were conducted using threaded steel bar with a diameter of 16 mm, and a total of four sets of pull-out specimens were used. The test variable was the length of the reinforcement anchorage, with anchorage lengths of 30 mm, 50 mm, 80 mm, and 100 mm considered. The test shows that the average bonding strength decreases as the anchorage length increases. The reason for this phenomenon is that the pull-out force of the specimen is closely correlated with the bonding area, and the bonding area also increases as the anchorage length increases, resulting in an increase in the pull-out force. However, the bonding mechanism analysis between ribbed steel bar and concrete reveals that as the anchorage length increases, the average bonding stress in the anchorage section decreases. Because the bonding stress distribution in the anchorage section is non-uniform, and a longer anchorage section will lead to a lower average bonding stress for a constant ultimate bonding stress. The experimental results of this study conform to this trend. The figure shows that as the anchorage length increases, the bonding strength gradually decreases. When the anchorage length is 30mm, the average bonding stress is 19.55 MPa. When the anchorage length is 50 mm, the average bonding stress is 16.47 MPa, reducing by 15.75 % compared to the 30 mm anchorage length. When the anchorage length is 80 mm, the average bonding stress is 13.33 MPa, which increases by 19.06 % compared to the 60 mm length. When the

anchorage length is 100 mm, the average bonding stress is 10.65 MPa, which increases by 20.11 % compared to the 70 mm length.

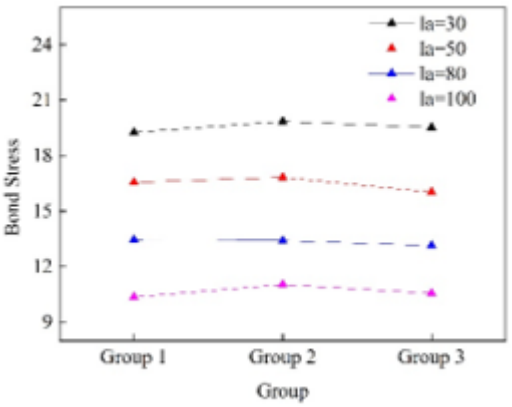

Figure 19. Comparison of bonding stress (Different anchorage lengths)

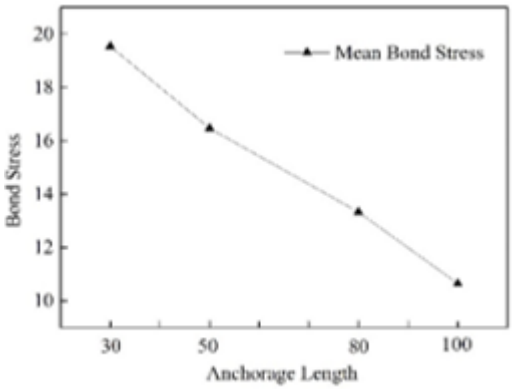

Figure 20. Average bonding stress diagram

3.6.3. Steel Reinforcement Diameter and Shape

Comparative chart of bond stress is shown in Figure 21, and average bond stress graph is shown in Figure 22. In the study, the impact of the diameter and shape of steel bar on its bonding strength with PUC material is studied. They tested different diameters of 12 mm, 16 mm, and 20 mm, with two shapes: ribbed steel bar and plain round steel bar. Through their experiments, the researchers observes that the bonding stress decreased as the diameter of the steel bar increases. The average bonding stress is 17.97 MPa for the diameter of 12 mm, 16.47 MPa for the diameter of 16 mm, and 13.5 MPa for the diameter of 20 mm. The plain round steel bar has a low bonding stress of 6.4 MPa, which is only 47.4 % of that of ribbed steel bar under the same conditions. The researchers attribute this difference to the mechanical interlocking property of ribbed steel bar and the frictional property of plain round steel bar. Overall, the study findings indicate that steel bar diameter and shape are critical factors that affect the bonding strength with PUC. The researchers recommend considering these factors in construction design and material selection to ensure the durability and stability of structures.

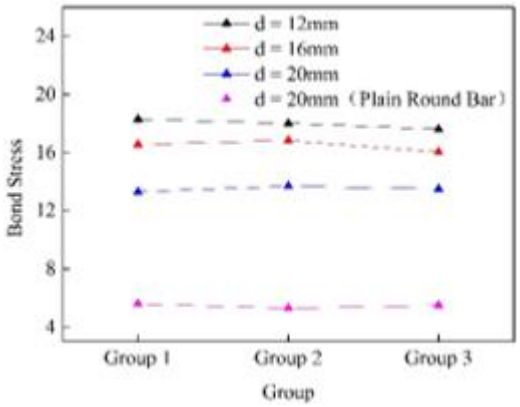

Figure 21. Comparative chart of bond stress (Different steel bar diameter)

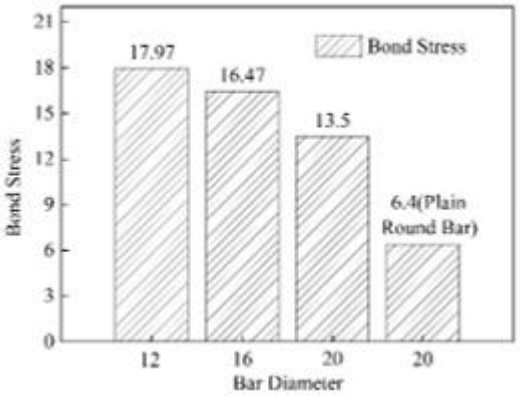

Figure 22. Average bond stress graph

Figure 23 illustrates a comparative chart depicting the bond stress. The average bond stress curve is depicted in Figure 24. For a 12 mm diameter steel bar, the measured stress is 14.37 MPa. When the steel bar diameter increases to 16 mm, the average bond stress decreases by 7.24% to 13.33 MPa in comparison to the 12 mm diameter steel bar. Similarly, for a 20 mm diameter steel bar, the average bond stress decreases by 9.45 % to 12.07 MPa when compared to the 16 mm diameter steel bar. Notably, the

measured bond stress for a smooth round steel bar with a 20 mm diameter is only 6.4 MPa, which amounts to 32.31 % of the bond stress exhibited by the ribbed steel bar under identical conditions. In summary, these findings suggest that the bond stress exhibits a decreasing trend as the diameter of the steel bar increases. Ribbed steel bars possess higher bond stress than smooth round steel bars under identical conditions. These results emphasize the significance of steel bar diameter and shape selection in ensuring the durability and stability of structures.

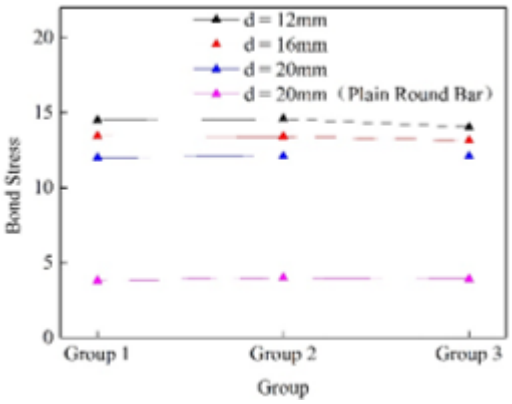

Figure 23. Comparative chart of bond stresses (Different anchorage lengths)

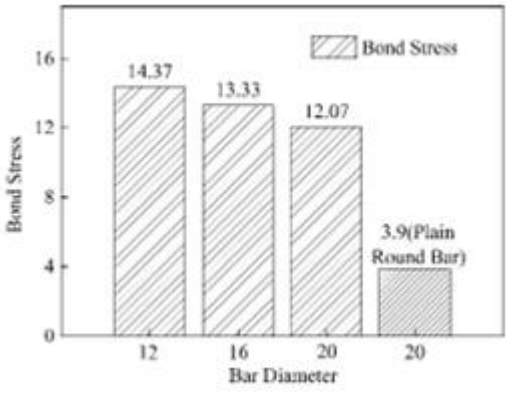

Figure 24. Average bond stress graph

4. Conlusions

In this paper, the axial tensile test of PUC material, the bonding property with concrete material, corrosion resistance, mechanical property at high temperature and the bonding property with steel bar are carried out. Findings are as follows:

The tensile strength of the PUC material is 31 MPa, and the constitutive relationship curve of bending-tensile stress-strain is derived by fitting. Additionally, the PUC material exhibits excellent resistance to chemical corrosion.

The bond strength between PUC material and concrete is measured at 3.56 MPa under axial loading, while it is 3.16 MPa under flexural loading. Bond tests have shown that interface failure occurs within the concrete material, suggesting that the PUC material exhibits strong bonding performance.

In axial tensile tests of PUC material conducted at various temperatures (-40 to 60°C), it has been observed that the ultimate strength of the material remains relatively stable in the temperature range of 40 to 60°C. However, at an elevated temperature of 60°C, there is a noticeable increase in tensile strain.

The bond strength between steel bars and PUC material is influenced by the protective layer thickness. As the thickness of the protective layer increases, the bond strength also increases. For example, when the protective layer thickness is 70 mm, the maximum measured bond stress is 16.38 MPa. On the other hand, the bond strength decreases with an increase in anchorage length. For a 100 mm anchorage length, the bond stress is 10.65 MPa, which is approximately 54.48% of the average bond stress observed at 30 mm. Moreover, smooth round steel bars exhibit significantly lower bond strength compared to deformed steel bars, with the former measuring around 47.4% of the bond strength of the latter under identical conditions.

References

1. MIYAMOTO, A., TEI, K., NAKAMURA, H., Behavior of prestressed beam strengthened with external tendons, *Journal of Structural Engineering*, 2000, 126(9): 1033-1044.
2. PARK, Y., H., PARK, C., PARK, Y., G., The behavior of an in-service plate girder bridge strengthened with external prestressing tendons, *Engineering Structures*, 2005, 27(3): 379-386.
3. REGGIA, A., MORBI, A., PLIZZARI, G., A., Experimental study of a reinforced concrete bridge pier strengthened with HPFRC jacketing, *Engineering Structures*, 2020, 210: 110355.

4. SCHNERCH, D., DAWOOD, M., RIZKALLA, S., Proposed design guidelines for strengthening of steel bridges with FRP materials, *Construction and Building Materials*, 2007, 21(5): 1001-1010.
5. HOU, P., YANG, J., PAN, Y., Experimental and simulation studies on the mechanical performance of concrete T-Girder bridge strengthened with K-Brace composite trusses, *Structures*, 2022, 43: 479-492.
6. OKEIL, A., M., EL-TAWIL, S., SHAHAWY, M., Flexural reliability of reinforced concrete bridge girders strengthened with carbon fiber-reinforced polymer laminates, *Journal of Bridge Engineering*, 2002, 7(5): 290-299.
7. HERBRAND, M., ADAM, V., CLASSEN, M., Strengthening of existing bridge structures for shear and bending with carbon textile-reinforced mortar, *Materials*, 2017, 10(9): 1099.
8. GRAYSON-WALLACE, B., ALJASAR, A., CHENG, L., Advances in Shear Strengthening of Concrete Bridge Girders, *Journal of Bridge Engineering*, 2022, 27(6): 03122002.
9. YANG, J., HOU, P., PAN, Y., Shear behaviors of hollow slab beam bridges strengthened with high-performance self-consolidating cementitious composites, *Engineering Structures*, 2021, 242: 112613.
10. CZADERSKI, C., MOTAVALLI, M., 40-Year-old full-scale concrete bridge girder strengthened with prestressed CFRP plates anchored using gradient method, *Composites Part B: Engineering*, 2007, 38(7-8): 878-886.
11. LEE, Y., S., WIPF, T., J., PHARES, B., M., Evaluation of steel girder bridge strengthened with carbon fiber–reinforced polymer posttension bars, *Transportation Research Record*, 2005, 1928(1): 232-244.
12. ZHANG, K., ZHU, X., CAO, Y., Experimental study on mechanical properties of polyurethane cement composite (PUC) under various temperatures, *Mater. Plast*, **60**(2), 2023, 32-42.
13. ALI, O., BIGAUD, D., FERRIER, E., Comparative durability analysis of CFRP-strengthened RC highway bridges, *Construction and Building Materials*, 2012, 30: 629-642.
14. LOPEZ, A., GALATI, N., ALKHRDAJI, T., Strengthening of a reinforced concrete bridge with externally bonded steel reinforced polymer (SRP), *Composites Part B: Engineering*, 2007, 38(4): 429-436.
15. GENTILE, C., SVECOVA, D., RIZKALLA, S., H., Timber beams strengthened with GFRP bars: development and applications, *Journal of Composites for Construction*, 2002, 6(1): 11-20.
16. AL-SAIDY, A., H., KLAIBER, F., W., WIPF, T., J., Parametric study on the behavior of short span composite bridge girders strengthened with carbon fiber reinforced polymer plates, *Construction and Building Materials*, 2008, 22(5): 729-737.
17. BENEBERU, E., YAZDANI, N., Residual strength of CFRP strengthened prestressed concrete bridge girders after hydrocarbon fire exposure, *Engineering Structures*, 2019, 184: 1-14.
18. HU, W., LI, Y., YUAN, H., Review of experimental studies on application of FRP for strengthening of bridge structures, *Advances in Materials Science and Engineering*, 2020, 2020: 1-21.
19. DEL, PRETE, I., BILOTTA, A., NIGRO, E., Performances at high temperature of RC bridge decks strengthened with EBR-FRP, *Composites Part B: Engineering*, 2015, 68: 27-37.
20. JOSEPH, R., MWAFY, A., ALAM, M., S., Seismic performance upgrade of substandard RC buildings with different structural systems using advanced retrofit techniques, *Journal of Building Engineering*, 2022, 59: 105155.
21. FU, T., WANG, K., ZHU, Z., Seismic performance of prefabricated square hollow section piers strengthened by jacketing using UHPC and high-strength steel, *Structures*, 2023, 47: 449-465.

Manuscript received: 04.01.2024